

Radio Polarization of BL Lacertae objects

Jun-Hui Fan^{1,2*}, Tong-Xu Hua¹, Yu-Hai Yuan¹, Yong-Xiang Wang³, Yi Liu¹,
Jiang-Bo Su¹, Yong-Wei Zhang¹, Jiang-He Yang⁴, Yong Huang¹

1. *Center for Astrophysics, Guangzhou University, Guangzhou 510006, China*

2. *Physics Institute, Hunan Normal University, Changsha, China*

3. *College of Science and Trade, Guangzhou University, Guangzhou 511442, China*

4. *Department of Physics and Electronics Science, Hunan University of Arts and Science, Changde 415000, China*

(Received ⟨reception date⟩; accepted ⟨acceptance date⟩)

Abstract

In this paper, using the database of the university of Michigan Radio Astronomy Observatory (UMRAO) at three (4.8 GHz, 8 GHz, and 14.5 GHz) radio frequencies, we studied the polarization properties for 47 BL Lacertae objects (38 radio selected BL Lacertae objects, 7 X-ray selected BL Lacertae, and two intermediate objects (Mkn 421 and Mkn 501), and found that (1) The polarizations at higher radio frequency is higher than those at lower frequency, (2) The variability of polarization at higher radio frequency is higher than those at lower frequency, (3) The polarization is correlated with the radio spectral index, and (4) The polarization is correlated with core-dominance parameter for those objects with known core-dominance parameters suggesting that the relativistic beaming could explain the polarization characteristic of BL Lacs.

Key words: BL Lacertae object, Polarization, Beaming Model

1. Introduction

BL Lacertae objects are generally described as a subclass of active galactic nuclei (AGNs), showing rapid and large amplitude variation, variable and high polarization, and core-dominated non-thermal continuum. Some BL Lacertae objects show superluminal motion and high energy gamma-ray emissions (Andruchow et al. 2005; Angel & Stockman 1980; Fan 2005; Fan et al. 1996; Gabuzda 2003; Gu et al. 2006; Gupta et al. 2004; Qian et al. 2003, 2004; Romero et al. 1995, 2002; Stickel et al. 1993; Tao & Qian, 2004; Wills et al. 1992; Xie et al. 2004).

According to the surveys, BL Lacertae objects can be divided into radio selected BL Lacertae objects (RBLs) and the X-ray selected BL Lacertae objects (XBLs). From the spectral energy distribution (SED), one can see that some BL Lacertae objects show lower-frequency peaked SED and are called as LBLs, while some others show higher-frequency peaked SED and are called as HBLs (see Urry & Padovani 1995 for a review). Generally, XBLs correspond to HBLs while RBLs to LBL. For Mkn 421 and Mkn 501, they are classified as RBLs by some and as XBLs by some other authors. However, from SED, they are both classified as HBLs.

The observational properties of RBLs are systematically different from those of XBLs. The latter have flatter spectral energy distribution from the radio through X-ray, a higher observed peak of the emitted power from radio through X-ray spectral energy distribution. Furthermore, RBL and XBL show different observation properties (see Angel & stockman 1980; Efimov, et al. 1988a,b, 2002;

Fan et al. 1997; Giommi et al. 1995; Junnuzi et al. 1994; Sambruna et al. 1996).

In this paper, we will investigate the radio properties of polarization in BL Lacertae objects based on the MURAO data base. It is arranged as follows. In section 2, we will calculate the averaged polarization and the variation of polarization for RBLs and XBLs. In section 3, we give some discussion and a conclusion.

2. Calculation and Results

From the MURAO data base, we can get 47 BL Lacertae objects, 38 of them are RBLs, 7 of them are XBLs, two of them (Mkn 421 and Mkn 501) are intermediate type. For those sources, we did following calculations

2.1. Radio Spectral Index

For each source, firstly we got its averaged flux densities at three radio frequencies (4.8GHz, 8.0GHz and 14.5 GHz) respectively, then adopted the linear regression analysis to the averaged flux at the three frequencies, we got the fitting result as $\log S_\nu = -\alpha \log \nu + c$. Therefore, we finally got the spectral index, α ($S_\nu \propto \nu^{-\alpha}$). The resulting spectral indexes are listed in Table 1, from which, we found that the radio spectral indexes for the 7 XBLs are in the range of $\alpha = -0.188$ to $\alpha = 0.625$ with an averaged value of $\langle \alpha \rangle = 0.235 \pm 0.255$ while those for the 38 RBLs are in the range of $\alpha = -0.601$ to $\alpha = 0.757$ with an averaged value of $\langle \alpha \rangle = 0.044 \pm 0.264$.

2.2. Radio Polarization

For the RBLs and XBLs, we calculated respectively the averaged maximum polarization and the averaged polar-

* email:fjh@gzhu.edu.cn

ization based on the observed polarization of each source. The detail procedure is as follows. At each frequency for each source, we chose the observed maximum polarization value as the maximum polarization at the corresponding frequency, and calculated the averaged value of the whole observation polarization as the averaged polarization. Therefore, we have three maximum polarizations and three averaged polarizations (at 4.8, 8.0 and 14.5 GHz) for each source. Then for each subclass (XBL and RBLs), we can calculate the averaged maximum polarization at frequency ν ($\nu = 4.8, 8.0$ and 14.5 GHz) $P_{\nu}^{Max} = \sum P_{i,\nu}^{Max} / N$, here $P_{i,\nu}^{Max}$ is the maximum observed polarization at frequency ν for the i th source in the subclass, and N is the source number of the subclass. $N = 7$ and 38 for XBLs and RBLs respectively. The averaged averaged polarization is also calculated as $P_{\nu}^{Ave} = \sum P_{i,\nu}^{Ave} / N$ here $P_{i,\nu}^{Ave}$ is the averaged observed polarization for the i th source in the subclass. So, we can get following statistical results.

$$\langle P_{4.80\text{GHz}}^{Max}(\%) \rangle = 36 \pm 29,$$

$$\langle P_{8.00\text{GHz}}^{Max}(\%) \rangle = 65 \pm 23,$$

$$\langle P_{14.5\text{GHz}}^{Max}(\%) \rangle = 74 \pm 25,$$

and

$$\langle P_{4.80\text{GHz}}^{Ave}(\%) \rangle = 7 \pm 5,$$

$$\langle P_{8.00\text{GHz}}^{Ave}(\%) \rangle = 16 \pm 7,$$

$$\langle P_{14.5\text{GHz}}^{Ave}(\%) \rangle = 17 \pm 7$$

for 7 XBLs,

$$\langle P_{4.80\text{GHz}}^{Max}(\%) \rangle = 17 \pm 13,$$

$$\langle P_{8.00\text{GHz}}^{Max}(\%) \rangle = 26 \pm 21,$$

$$\langle P_{14.5\text{GHz}}^{Max}(\%) \rangle = 29 \pm 21,$$

and

$$\langle P_{4.80\text{GHz}}^{Ave}(\%) \rangle = 4 \pm 2,$$

$$\langle P_{8.00\text{GHz}}^{Ave}(\%) \rangle = 5 \pm 3,$$

$$\langle P_{14.5\text{GHz}}^{Ave}(\%) \rangle = 6 \pm 3$$

for 38 RBLs.

2.3. Results

For polarization, the averaged results suggest that both the maximum and averaged polarizations increase with the radio frequency in the radio range of from 4.8GHz to 14.5GHz. In addition, within that radio frequency range both the averaged maximum and the averaged average polarization in XBLs are higher than those in RBLs at the same radio frequency.

For the polarization and the spectral index, there is a tendency for the radio polarization to increase with the spectral index for BL Lacertae objects as shown in Fig. 1

The core-dominance parameter is an important parameter calculated from the radio observation. It is defined as

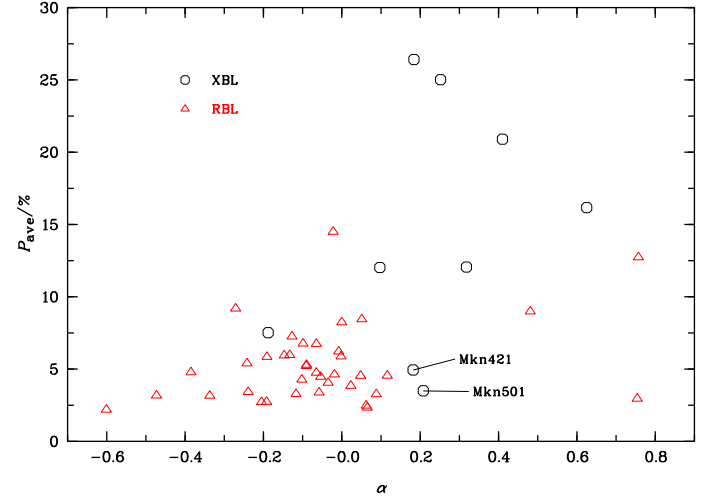


Fig. 1. The relation between the averaged polarization at 8 GHz and the radio spectral index for radio selected BL Lacertae objects–RBL (triangles) and X-ray selected BL Lacertae objects–XBL (open circles)

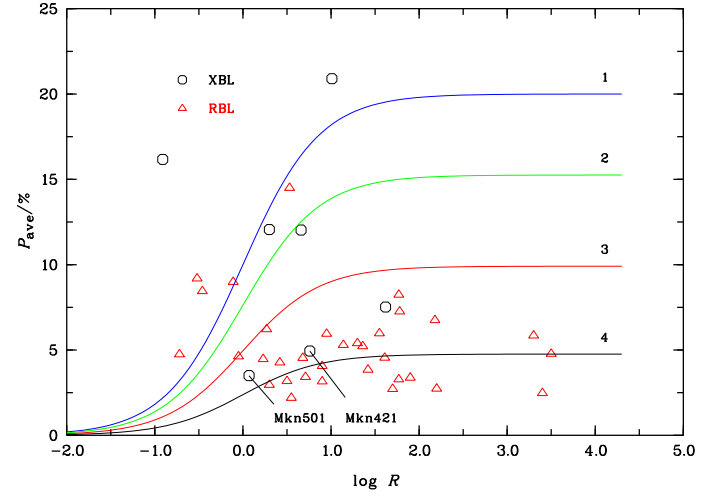


Fig. 2. The relation between the averaged polarization at 8 GHz and the core-dominance parameter for radio selected BL Lacertae objects–RBL (triangles) and X-ray selected BL Lacertae objects–XBL (open circles). Curve 1 stands for $\eta = 0.25$, curve 2 stands for $\eta = 0.18$, curve 3 stands for $\eta = 0.11$, and curve 4 stands for $\eta = 0.05$.

the ratio of the core flux density to the extended flux density (Orr & Browne 1982). For polarization and the core-dominance parameter, we plotted the averaged 8GHz polarization against the core dominance parameter as shown in Fig. 2.

3. Discussion

It is believed that the particular properties observed from BL Lacertae objects are associated with the beaming effect, and the beaming model was adopted to explain

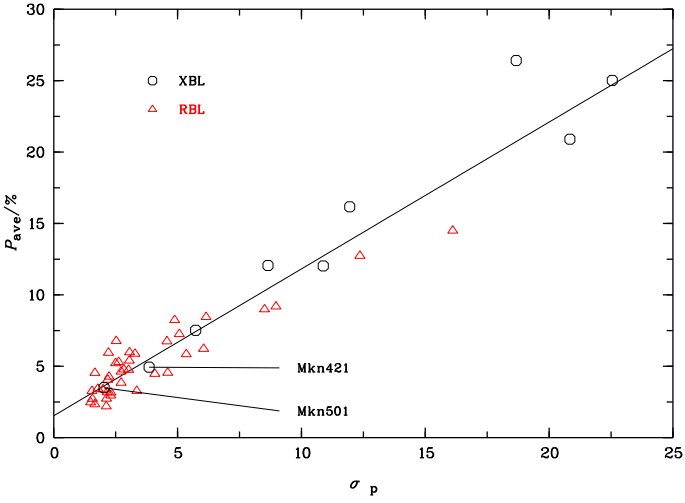


Fig. 3. The relation between the averaged polarization at 8 GHz and the polarization variability- σ_P for radio selected BL Lacertae objects-RBL (triangles) and X-ray selected BL Lacertae objects-XBL (open circles). The line stands for the best fitting result.

both the particular observational properties and some observational differences between RBLs and XBLs (see Fan et al. 1997; Fan & Xie 1996; Georganopoulos & Marscher 1999) although the viewing angle alone can not explain all the difference between RBLs and XBLs (Sambruna et al. 1996).

High and variable polarization is one of the characteristics of BL Lacertae objects. For the radio polarization, although the averaged value indicates that the polarization in XBLs is higher than that in RBLs, we can get the conclusion that the radio polarization in XBLs is not always higher than that in RBLs. The reasons are that 1) There are only 7 XBLs in our consideration, and 2) for the sources with the averaged polarization being higher than 10%, we have two RBLs but 6 XBLs. However, for the sources with maximum polarization being higher than 35%, we have 9 RBLs but 3 XBLs. We think that whether or not the radio polarization in XBLs is higher than that in RBLs, more radio polarization observations are significant and encouraged.

When we take into account of the polarization variation, we can use the standard deviation, σ_P as the variation indication. In this sense, we found that the variation is closely linearly correlated with the averaged polarization shown in Fig. 3, the line stands for the best fitting result, $P_{ave}(\%) = (1.02 \pm 0.04)\sigma_P + (1.54 \pm 0.32)$. Here we used the data at 8GHz.

When we considered the relationship of polarization on the spectral index, we found that the radio polarization increases with the spectral index, α ($S_\nu \propto \nu^{-\alpha}$). The data can give a linear relation of $P \sim 9.15\alpha + 7.04$. From the synchrotron emission, one can get that the polarization is proportional to $\frac{\alpha+1}{\alpha+5/3}$, which suggests that the polarization is correlated with the spectral index and that the

polarization increases with the spectral index. Although our statistical result show a trend that the polarization increase with the radio spectral index as shown in Fig. 1, the trend is largely different from the prediction by synchrotron emission.

Polarization is found to be associated with the core-dominance parameter (see Wills et al. 1992 and reference therein) with high polarization corresponding to large $\log R$. For the present sample, one can get a plot of the radio polarization against the core-dominance parameter as shown in Fig. 2. In Fig. 2, we only showed the averaged radio polarization at 8.0GHz and the core dominance parameters that are available in the literature.

Based on the two-component beaming model Urry & Shafer (1984) (see also Urry & Padovani, 1995), the emissions of an AGN are from two components, namely the beamed and the unbeamed ones. Assuming the intrinsic flux of the jet, S_j^{in} , to be a fraction f of the unbeamed flux, S_{unb} , i.e., $S_j^{in} = fS_{unb}$, one can get $S^{ob} = S_{unb} + S_j^{ob} = (1 + f\delta^p)S_{unb}$. If one assumes that the emissions in the co-moving jet are also composed of two components, namely the polarized and the unpolarized, with the two components being proportional to each other, $S_j^{in} = S_j^p + S_j^{up}$, $S_j^p = \eta S_j^{up}$. Then a relation between the observed polarization and the Doppler factor can be obtained (Fan et al. 1997; see also Fan et al. 2001).

$$P^{ob} = \frac{(1+f)\delta^p}{1+f\delta^p} P^{in} \quad (1)$$

where P^{in} is the intrinsic polarization expressed in the form

$$P^{in} = \frac{f}{1+f} \frac{\eta}{1+\eta} \quad (2)$$

which follow

$$P^{ob} = \frac{f\delta^p}{1+f\delta^p} \frac{\eta}{1+\eta} \quad (3)$$

δ is the Doppler factor, η is the ratio of the polarized to the unpolarized luminosity in the jets. The value of p depends on the shape of the emitted spectrum and the detailed physics of the jet (Lind & Blandford 1985), $p = 3 + \alpha$ is for a moving sphere and $p = 2 + \alpha$ is for the case of a continuous jet, α is the spectral index.

If we use the expression for the core-dominance parameter, $R = f((\Gamma(1 - \beta \cos\theta))^{-p} + (\Gamma(1 + \beta \cos\theta))^{-p}) = f\delta^p[1 + f(\frac{1 - \beta \cos\theta}{1 + \beta \cos\theta})^p]$, then the polarization can be written in the form

$$P^{ob} = \frac{R - G(f, \theta, \beta)}{1 - G(f, \theta, \beta) + R} \frac{\eta}{1 + \eta}, \quad (4)$$

here, $G(f, \theta, \beta) = f(\frac{1 - \beta \cos\theta}{1 + \beta \cos\theta})^p$. Since the observed polarization is positive, then we can get the value of $G(f, \theta, \beta)$ to be smaller than the value of R . Therefore, the value of $G(f, \theta, \beta)$ is actually very small since the $\log R$ is -0.91 for 1100+772. So, we have

$$P^{ob} \sim \frac{R}{1+R} \frac{\eta}{1+\eta}. \quad (5)$$

For a given η , a theoretical relation of polarization depending on the core-dominance parameter can be obtained. In Fig. 2, we showed the polarization vs core-dominance parameter plot. The core-dominance parameter is taken as the jet viewing indication, it is actually the indication of a beaming effect. For a strongly boosted source, the core-dominance parameter can be simply expressed as $R = f\delta^p$ (Ghisellini et al. 1993). In this sense, one can see clearly that 1) the polarization is consistent with the explanation that the polarization is associated with the beaming effect and 2) for most sources, their η is less than 0.25.

In this paper, based on the MURAO data base, we considered the radio polarization for BL Lacertae objects and found that the averaged polarization depends on the frequency, the spectral index and the core-dominance parameter. The polarization variation is closely correlated with the polarization. The relativistic beaming could explain the polarization characteristic of BL Lacs.

4. Acknowledgements

We thank the referee for the useful comments and suggestions. This work is partially supported by the National 973 project (NKBRSF G19990754), the National Science Fund for Distinguished Young Scholars (10125313), the National Natural Science Foundation of China (10573005,10633010), and the Fund for Top Scholars of Guangdong Province (Q02114). We also thank the financial support from the Guangzhou Education Bureau and Guangzhou Science and Technology Bureau. This research has made use of data from the University of Michigan Radio Astronomy Observatory which has been supported by the University of Michigan and the National Science Foundation.

References

Andruchow, I., Romero, G. E., Cellone, S. A., 2005, A&A, 442, 97

Angel J.R.P. & Stockman H.S., 1980, ARA&A 8, 321

Efimov Y. & Shakhovskoy N.M. 1988a, OJ-94 annual meeting 1997 "Multifrequency monitoring of Blazars", Publ. Ossrv. Astro. Univ. di Perugia, 3. 24

Efimov Y. & Shakhovskoy N.M., 1988b, BLAZAR DATA, 1. No 3.

Efimov Y.S., Shakhovskoy N.M., Takalo L.O., Sillanpaa, A. 2002, A&A, 381, 408,

Fan J.H, 2005, ChJAA, 5S, 213

Fan, J.H., & Zhang, J.S., 2003, A&A, 407, 899

Fan, J.H., Cheng, K. S., Zhang, L. 2001, PASJ, 53, 201

Fan J.H., Xie G.Z., Pecontal E., et al., 1998, ApJ 507, 173

Fan J.H., Cheng K.S., Zhang L., Liu C., 1997, A&A 327, 947

Fan J.H., Xie G.Z., Wen S.L., 1996, A&AS 116, 409

Fan J.H., Xie G.Z., 1996, A&A 306, 55

Gabudza, D.C., 2003, ApSS, 288, 39

Georganopoulos M., Marscher A.P., 1999, ASP Conf. Vol. 159

Ghisellini G., Padovani P., Celotti A., Maraschi L., 1993, ApJ 407, 65

Giommi P., Ansari S.A., Micol A., 1995, A&AS 109, 267

Gu, M.F., Lee1, C.-U., Pak1,S., Yim1, H. S. , Fletcher, A. B. 2006, A&A, (accepted)(astro-ph/0602180)

Gupta, A.C., Banerjee, D.P.K., Ashok, N.M., Joshi, U.C., 2004, A&A, 422, 505

Jannuzzi B.T., Smith P.S., Elston R., 1994, ApJ 428, 130

Lind K.R. & Blandford R.D., 1985, ApJ 295, 358

Orr, M. J. L., Browne, I. W. A., 1982, MNRAS, 200, 1067

Qian, B. C., Tao, J., 2003, PASP, 115, 490

Qian, B. C., Tao, J., 2004, PASP, 116, 161

Romero C.E., Combi J.A., Vucetich H., 1995, ApSS 225, 183

Romero, G. E., Cellone, S. A., Combi, J. A., Andruchow, I., 2002, A&A, 390, 431

Sambruna R., Maraschi L., Urry C.M., 1996, ApJ 463, 444

Stickel M., Fried J.W., Kuhr H., 1993, A&AS 98, 393

Takalo L.O., 1994, VA 38, 771

Tao, J., Qian, B.C. 2004, PASP, 116, 634

Urry C.M., & Padovani P., 1995, PASP 107, 803

Urry C.M. & Shafer R.A., 1984, ApJ 280, 569

Wills B.J., Wills D., Breger M., 1992, ApJ 398, 454

Xie, G.Z., et al. 2004, MNRAS, 348, 831

Table 1. A sample of 47 BL Lacertae objects

Source	Class	α	P_{8GHz}^{ave}	σ_p	Data span	$\log R$	Ref
0003-066	RBL	0.088	3.27	1.54	1978-1998		
0048-097	RBL	-0.242	5.4	3.05	1970-1999	1.3	G93
0109+224	XBL	-0.188	7.52	5.73	1978-1999	1.62	W92
0215+015	RBL	-0.337	3.16	2.31	1979-1999	0.9	W92
0219+428	RBL	0.754	2.96	2.3	1974-1999	0.3	G93
0235+164	RBL	-0.192	2.74	2.13	1974-1999	2.2	G93
0300+470	RBL	-0.058	3.38	1.99	1975-1999	1.9	G93
0323+022	XBL	0.252	25.02	22.55	1985-1999		
0422+004	RBL	-0.191	5.85	5.35	1978-1999	3.3	W92
0716+714	RBL	-0.271	9.19	8.97	1981-1999	-0.52	W92
0735+178	RBL	0.062	2.48	1.49	1977-1999	3.4	G93
0754+100	RBL	-0.09	5.3	2.62	1978-1999	1.14	W92
0808+019	RBL	-0.133	5.98	3.06	1979-1999	1.55	W92
0814+425	RBL	-0.035	4.06	2.18	1977-1999	0.9	W92
0818-128	RBL	-0.054	4.47	4.08	1979-1999	0.23	W92
0829+046	RBL	-0.239	3.42	1.78	1978-1999	0.71	F03
0851+202	RBL	-0.385	4.78	2.83	1971-1999	3.5	G93
0912+297	XBL	0.318	12.06	8.65	1980-1999	0.3	W92
0954+658	RBL	-0.022	14.5	16.11	1974-1999	0.53	W92
0957+227	RBL	0.757	12.74	12.36	1979-1999		
1100+772	XBL	0.625	16.17	11.95	1983-1999	-0.91	W92
1101+384	Mid-BL	0.182	4.94	3.85	1978-1999	0.76	F03
1133+704	XBL	0.184	26.41	18.67	1980-1999		
1147+245	RBL	0.023	3.85	2.72	1979-1999	1.42	W92
1215+303	RBL	-0.008	6.22	6.05	1979-1999	0.27	W92
1219+285	RBL	-0.065	4.75	3.02	1978-1999	-0.72	F03
1307+121	RBL	-0.002	5.88	3.28	1978-1999		
1308+326	RBL	-0.205	2.72	1.56	1976-1999	1.7	G93
1400+162	RBL	0.481	8.99	8.51	1978-1999	-0.11	F03
1413+135	RBL	-0.601	2.2	2.12	1978-1999	0.55	F03
1418+546	RBL	-0.117	3.28	3.35	1978-1999	1.77	W92
1514+197	RBL	-0.065	6.75	4.57	1978-1999	2.18	W92
1538+149	RBL	-0.147	5.95	2.21	1977-1999	0.95	W92
1652+398	Mid-BL	0.208	3.5	2.03	1977-1999	0.07	F03
1717+178	RBL	-0.127	7.26	5.07	1977-1999	1.78	W92
1727+502	XBL	0.41	20.9	20.84	1979-1999	1.01	W92
1749+096	RBL	-0.473	3.18	2.15	1978-1999	0.5	F03
1749+701	RBL	0.051	8.45	6.15	1980-1999	-0.46	F03
1803+784	RBL	-0.102	4.27	2.23	1981-1999	0.42	F03
1807+698	RBL	0.048	4.54	1.66	1979-1999	0.68	F03
1823+568	RBL	-0.099	6.77	2.52	1981-1999		
2007+777	RBL	-0.091	5.22	2.5	1981-1999	1.36	G93
2032+107	RBL	0.116	4.55	4.6	1978-1999	1.61	W92
2131-021	RBL	0.065	2.34	1.66	1974-1999		
2155-304	XBL	0.097	12.03	10.88	1979-1999	0.66	W92
2200+420	RBL	-0.019	4.63	2.72	1968-1999	-0.05	F03
2254+074	RBL	0	8.24	4.88	1979-1999	1.77	W92

Note to the Table: Col. 1 gives the name of the source, Col. 2 the classification, XBL is for X-ray selected BL Lacertae object, RBL for radio selected BL Lacertae object while mid-term for the object between XBL and RBL, Col. 3 for the spectral index($S_\nu \propto \nu^{-\alpha}$), Col. 4 for the averaged observation polarization at 8GHz, Col. 5 for the 1 σ deviation of the averaged polarization in Col. 4, Col. 6 for the time span of the observation data, Col. 7 for the core-dominance parameter, Col. 8 reference for the core-dominance parameter in Col. 7, respectively.

F03: Fan & Zhang (2003); G93: Ghisellini et al. (1993); W92: Wills et al. (1992)